A Ni(COD)$_2$-Free Approach for the Synthesis of High Surface Area Porous Aromatic Frameworks

SCHOLARONE™
Manuscripts

COMMUNICATION

A Ni(COD)$_2$-Free Approach for the Synthesis of High Surface Area Porous Aromatic Frameworks

Anthony J. Porath,[a] Malsha A. Hettiarachchi,[a] Shuxiao Li,[a] James R. Bour[a],*

Abstract: Porous aromatic frameworks (PAFs) are attractive materials for applications where high surface area and material stability govern performance. Most of the highest surface area PAFs are synthesized using poorly scalable and costly methods involving super-stoichiometric bis(1,5-cyclooctadiene)Nickel(0) (Ni(COD)$_2$). This communication describes a general approach for the synthesis of high surface area PAFs that does not use isolated Ni(COD)$_2$. The method is general to at least seven microporous polymers and can be conducted on gram scales without the use of an inert atmosphere glovebox. This work is expected to improve the synthetic accessibility of these materials.

Porous aromatic frameworks are network polymers that are typically constructed through irreversible polymerization of rigid, primarily aromatic multidimensional monomers.[1,2] The strong bonds between light atom monomer units and rigid linkages in the polymer often endow these materials with both broad-spectrum chemical stability and high surface areas.[1–6] Since Zhu's seminal report on high surface area PAF-1 in 2009,[7] multiple PAFs with Brunauer-Emmet-Teller surface areas (SA$_{BET}$) in excess of 3500 m^2 g^{-1} have been reported. [5,8–10] Many of these materials are stable to strong acid, base, and temperatures above 350 °C. Their combined high surface area and stability render them promising candidates for applications where porosity and material stability govern performance. PAFs are currently under investigation for applications in gas storage/purification,[9,11–14] water purification,[15–17] energy storage,[18–21] and catalysis.[22–25] Their excellent figures of merit in many these applications are often attributed to their high stability and/or high surface areas.

Most of the highest surface area PAFs are synthesized through organometallic coupling reactions.[1,2,4,9,10] Organometallic reactions are well-suited to couple the high sp^2 and sp content motifs monomers comprising most PAFs. Among these approaches, nickel-mediated aryl electrophile homocoupling reactions, also known as Yamamoto-type Ullmann homocouplings, consistently dominate synthetic approaches for the highest surface area PAFs.[1] Porous aromatic framework syntheses based on this reaction generally rely on 1-2 equivalents of Ni(COD)$_2$ per C-X bond of the aryl electrophile monomer to mediate PAF formation.[4,5,9,10,14] This method reliably yields more porous PAFs than other synthetic approaches (e.g. Suzuki polymerizations, organic condensation reactions).[7,17,26]

The superiority of nickel-mediated aryl electrophile homocouplings relative to other methods has been attributed, at least in part, to the high efficiency with which Ni^0/ligand complexes insert into monomer C-X bonds.[2,4,27] This reaction precedes the key C-C bond-forming reaction and also dehalogenates the monomer, reducing overall polymer density.[28] Starting from well-defined Ni^0 precursors such as Ni(COD)$_2$ ensures efficiency in this key step, but at significant limitation to scale, economy, and overall accessibility of these materials. Ni(COD)$_2$ is costly, acutely air sensitive, and still difficult to synthesize on large scales, though recent advances have improved its synthesis.[29] Porous aromatic framework syntheses based on nickel-mediated electrophile couplings generally require an inert atmosphere glovebox and are typically conducted on scales less than 0.5 g. These challenges ultimately limit the accessibility and scalability of these materials for those exploring PAF applications.
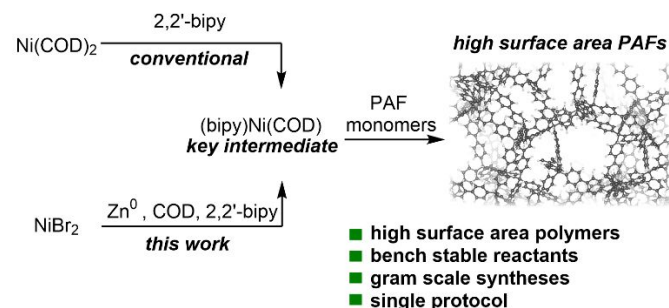
Scheme 1. Overview of this work

We hypothesized that in situ reduction of air stable nickel salts is a potential alternative to Ni(COD)$_2$-based approaches. In situ reduction of NiX$_2$ compounds is effective in other nickel-mediated electrophile homocoupling polymerizations

a. *Department of Chemistry, Wayne State University, 5101 Cass Avenue, Detroit, MI 48202, USA.*

of non-porous polymers but has not been adapted to the unique challenges of PAF synthesis.[30–32] In this communication we describe a unified, Ni(COD)$_2$-free approach for the synthesis of high surface area PAFs. We show that simple activated Zn dust and NiBr$_2$ used in conjunction with 2,2'-bipyridine (bipy) and 1,5-cyclooctadiene (COD) are effective substitutes for isolated Ni(COD)$_2$ used in conventional nickel-mediated PAF syntheses. The method utilizes bench stable reagents, is general to at least seven polymers, and affords materials with overall comparable porosities to conventional approaches. Finally, we demonstrate that this protocol can be adapted to the gram-scale synthesis of prototypical high surface area PAF, PAF-1, without the use of an inert atmosphere glovebox.

We anticipated that judicious choice of reductant would be key to realization of the proposed approach. In situ formation of the active mediator poses at least two challenges. First, PAF surface areas are noted to be somewhat variable, suggesting that porosity may be sensitive to contaminants and/or small changes in conditions.[4,16,33] The addition of other reactants has potential to significantly affect product PAF porosity. Secondly, most PAFs are insoluble. Excess reagents and all reaction byproducts must be removed through washes for the isolation of pure, highly porous PAFs.
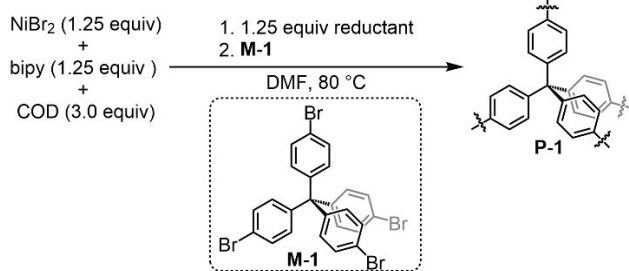
With these considerations in mind, we first examined the synthesis of prototypical high surface area PAF, PAF-1 (P-1), using inexpensive reductants and (bipy)NiBr$_2$ (formed in situ). We initially focused our studies on Mg^0, Mn^0, Zn^0, or (tetrakis(dimethylamino)ethylene) (TDAE) reductants because these reductants are known to reduce Ni^{II} salts to Ni^0, are reasonably expected to wash out in the conventional acidic workup, and have been employed in nickel-catalyzed small molecule electrophile couplings.[34–37] Upon addition of these reductants to the DMF solution of (bipy)NiBr$_2$, the solution turned the characteristic purple of (bipy)Ni^0 complexes.[38] This color quickly faded after addition of tetrakis(4-bromophenyl)methane (M-1) and returned after 10 minutes to 2 hours of additional stirring. The reactions were stirred at 80 °C for 18 hours after monomer addition before being quenched with a conventional acidic workup.[4,16] Under these conditions only activated Zn dust and Mg powder yielded the characteristically insoluble P-1 in sufficient quantities for characterization.

The surface area of P-1 made using Mg and Zn reductants was inferior to conventional approaches. Nitrogen adsorption isotherms at 77 K yielded BET surface areas of 1374 and 3482 m^2 g^{-1} using Mg and Zn reductants respectively (Table 1, entries 2 and 3). Though these are still highly porous, P-1 is typically synthesized with SA$_{BET}$ between 4100-5600 m^2 g^{-1}.[4,16,33,39] Attempts to improve the product polymer surface area through variation of concentration, solvent, other nickel salts, and temperatures were unsuccessful. Optimization efforts yielded comparable or worse micropore volumes and surface areas.

We next considered the possibility that the divalent oxidation products, ZnBr$_2$, MgBr$_2$, and MnCl$_2$ were poisoning the reaction. We hypothesized that they could compete for coordination to the bipy ligand in solution in sufficient equilibrium to negatively influence polymerization.[40–42] To attenuate potential interference of non-nickel M^0/M^{II} species

in solution through competitive coordination to bipy, the standard reactions were next run in the presence of 2.0 equivalents of 2,2-bipyridine relative to NiBr$_2$ (2.5 equivalents to C-Br). Under these conditions, all three metal reductants exhibited increased yield and surface area of the product polymers (Table 1 entries 7, 8, 9). The organic reductant, TDAE, still did not afford isolable polymer even with added bipy. Among the reductants evaluated, activated zinc dust performed the best. An average BET surface area of 4940 m^2 g^{-1} was measured as determined through N$_2$ adsorption isotherms at 77K. This result was consistent over two trials using different batches of M-1 (Table 1, entry 7). The surface area of P-1 synthesized through this route is comparable to reported surface areas of P-1 synthesized in our laboratory (Table 1, entry 1) as well as values published by other groups (4100-5600 m^2 g^{-1}) using conventional Ni(COD)$_2$.[4,16,33,39] Further increasing the stoichiometry to 3.75 equivalents to C-Br bonds of bipy had a minimal effect (Table 1, entry 12). Notably, addition of another equivalent of bipy to conventional Ni(COD)$_2$ protocols had the opposite effect on P-1 porosity. A reduction to SA$_{BET}$ 3766 m^2 g^{-1} from 4651 m^2 g^{-1} was observed. This observation suggests that the beneficial effect of added bipyridine is due to attenuated poisoning effects of the metal reductants and/or reductant byproducts. We tentatively propose that competitive coordination of MX$_2$ to 2,2'-bipyridine reduces polymerization efficiency, an effect apparently mitigated by increasing bipyridine stoichiometry relative to nickel.[43]

Table 1. Optimization of P-1 using exogenous reductant [a]

Entry	Reductant/Change from Standard [a]	SA$_{BET}$ (m^{2}g^{-1})
1	Ni(COD)$_2$ instead of NiBr$_2$	4651
2	Activated Zn dust/none	3482
3	Mg powder/none	1374
4	Mn powder/none	[b]
5	TDAE /none	[b]
6	Zn/Ni(OAc)$_2$ instead of NiBr$_2$	[b]
7	**Zn/ 2.5 equiv bipy instead of 1.25 equiv**	4940[c]
8	Mg/ 2.5 equiv of bipy instead of 1.25 equiv	3076
9	Mn/2.5 equiv bipy instead of 1.25 equiv	2759
10	TDAE/ 2.5 equiv bipy instead of 1.25 equiv	[b]
11	Zn/1.5 equiv bipy instead of 1.25 equiv	4181
12	Zn/3.75 equiv bipy instead of 1.25 equiv	5058
13	Zn/NMP, 2.5 equi bipy instead of DMF and 1equiv bipy	3198
14	Zn/DMAc, 2.5 equiv bipy instead of DMF and 1.25 equiv bipy	4618

[a]Stoichiometry reported relative to C-Br bonds [b]No polymer isolated through standard work-up. [c]Average of two polymerizations

The product PAFs made through the conditions in table 1, entry 7 (Method A) were overall similar to those made using conventional $Ni(COD)_2$ in our lab , Method B (Figure 1). Nitrogen adsorption isotherms at 77 K show similar overall uptake and pore size distributions (Figure 1a and 1b). Method A appears to yield materials with slightly larger pore volumes in the range of 1.5 to 2.0 nm than Method B when using NLDFT carbon slit models of pore size. The overall similar porosity was further corroborated by CO_2 adsorption isotherms 273 K. Slightly higher CO_2 adsorption up to 800 mmHg was noted in **P-1** prepared through Method B (Figure 1c). This slight increase in CO_2 uptake may be due the smaller average pore sizes, as has been noted in closely related PAFs.[14]
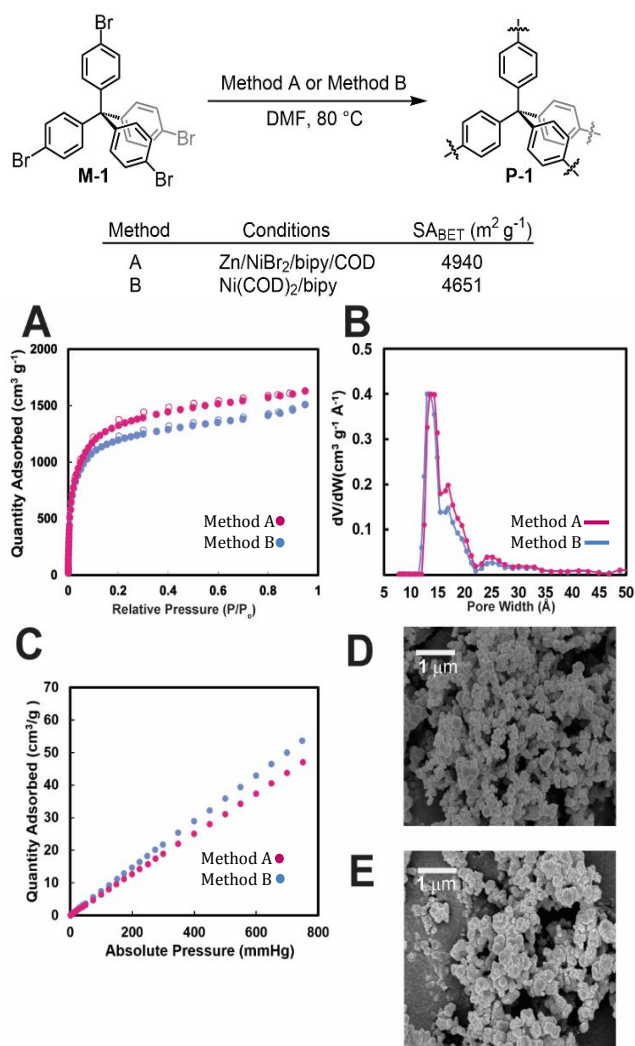

Figure 1. (A) Nitrogen adsorption (filled circles) and desorption (hollow circles) isotherms at 77 K (B) NLDFT pore size distributions (C) CO_2 isotherms at 273 K (D) SEM micrograph of **P-1** made through Method A (E) SEM image of **P-1** made through Method B.

The morphology and composition of **P-1** prepared through methods A and B was also similar. Scanning electron microscope images depict comparable morphologies and particle sizes (Figure 1d and 1e). Consistent with previous reports,[4,33] **P-1** forms clustered aggregates with most particles below 500 nm in size. Additional characterization by thermogravimetric analysis and elemental analysis also corroborate their overall similarity as well as low residual metal content (Figure S28 and Table S3 ESI).

To test if this approach is general to other PAFs, we evaluated the performance of Method A in the polymerization of six other structurally distinct monomers (**M2** –**M7,** figure 2).[3,5,10,14,44] These monomers span different dimensionalities, branch functionalities, and size. To benchmark the results against conventional $Ni(COD)_2$-based approaches, these monomers were also polymerized using Method B. As shown in table 2, Method A yields polymers with similar surface areas and pore volumes as Method B. In only two cases was a difference in surface area and overall pore volume of greater than 10% observed. Method A consistently outperformed Method B in the synthesis of **P-2** from **M-2**, yielding surface areas of 4773 $m^2\ g^{-1}$ and 4225 $m^2\ g^{-1}$, respectively. Only in the polymerization of **M-3** did Method B significantly outperform Method A (entries 5 and 6). Overall, Method A performs similarly to Method B, showing that it is not only a lower cost strategy for high surface area PAF synthesis but also general to at least seven PAFs.
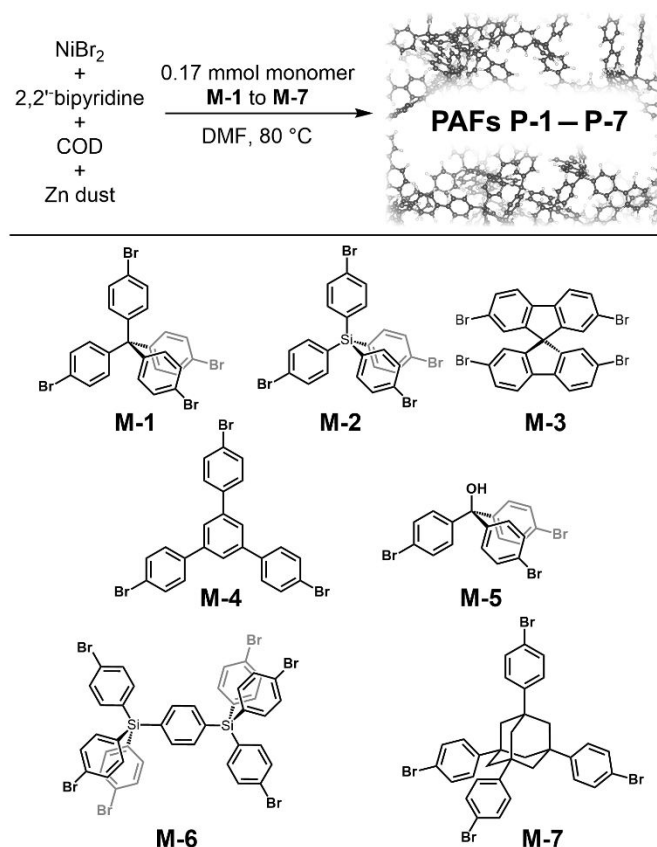

Figure 2. Monomers used for scope benchmarking studies between Method A and Method B

In a final set of experiments, we sought to translate this approach to a glovebox-free synthesis of **P-1** (Method C). We reasoned that the acute sensitivity of these reactions to adventitious oxygen would be partially attenuated by the extra reductant used in this approach.[16] After slight modification of Method A to accommodate gram scale solids addition on a Schlenk line (figure S2), **P-1** was synthesized in 89% yield based on theoretical structure with a BET surface area of 4450 $m^2\ g^{-1}$. Though this is lower than the average for Method A, it is well within the range typically reported for **P-**

1.[4,16,33,39] The composition was also similar based on elemental analysis (Table S3). Importantly, the reaction was conducted with reagents stored on the bench and with common commercially available anhydrous solvents, making this approach accessible to those without inert atmosphere gloveboxes.

Table 2. Optimization of **P-1** using exogenous reductant.

Entry	PAF	Method	SA_{BET} $(m^2 g^{-1})$	V_{tot} $(cm^3 g^{-1})^a$
1	**P-1**	A	4940[b]	2.50
2		B	4651	2.34
3	**P-2**	A	4773	2.63
4		B	4225	2.37
5	**P-3**	A	1595	1.43
6		B	2237	1.76
7	**P-4**	A	2042	1.93
8		B	2313	1.58
9	**P-5**	A	1386	0.77
10		B	1423	0.81
11	**P-6**	A	3968	2.16
12		B	3947	2.06
13	**P-7**	A	2440	1.60
14		B	2340	1.51

[a] Total pore volume based on single point pore volume at $p/p_0 =0.95$. [b] Average of two polymerizations.

In conclusion, this communication describes the directed development of a general, $Ni(COD)_2$-free approach for the synthesis of PAFs using nickel mediated electrophile homocoupling reactions. We show that the combination of simple nickel salts and activated Zn dust is a viable alternative to conventional $Ni(COD)_2$ if poisoning effects of Zn/ZnX_2 are mitigated by increasing the stoichiometry of 2,2-bipyridine. The resulting method can be carried out on the bench without the need for an inert atmosphere glovebox. We anticipate that this strategy will significantly increase the accessibility of these materials for non-experts and thereby accelerate the exploration of PAFs in targeted applications.

Conflicts of interest

The authors have no conflicts of interest to declare.

Notes and references

1   Y. Tian and G. Zhu, *Chem. Rev.*, 2020, **120**, 8934–8986.
2   S. Ben, Teng; Qiu, *CrystEngComm*, 2013, **15**, 17–26.
3   J. Schmidt, M. Werner and A. Thomas, *Macromolecules*, 2009, **42**, 4426–4429.
4   T. Ben, H. Ren, S. Ma, D. Cao, J. Lan, X. Jing, W. Wang, J. Xu, F. Deng, J. M. Simmons, S. Qiu and G. Zhu, *Angew. Chemie - Int. Ed.*, 2009, **48**, 9457–9460.
5   D. Yuan, W. Lu, D. Zhao and H. Zhou, *Adv. Mater.*, 2011, **23**, 3723–3725.
6   B. G. Hauser, O. K. Farha, J. Exley and J. T. Hupp, *Chem. Mater.*, 2013, **25**, 12–16.
7   Y. Yuan, F. Sun, H. Ren, X. Jing, W. Wang, H. Ma, H. Zhao and G. Zhu, *J. Mater. Chem.*, 2011, **21**, 13498–13502.
8   W. Lu, D. Yuan, D. Zhao, C. I. Schilling, O. Plietzsch, T. Muller, S. Bräse, J. Guenther, J. Blümel, R. Krishna, Z. Li and H. C. Zhou, *Chem. Mater.*, 2010, **22**, 5964–5972.
9   J. Jia, Z. Chen, J. Jia, Z. Chen, H. Jiang, Y. Belmabkhout and G. Mouchaham, *Chem*, 2019, 180–191.
10 M. Li, H. Ren, F. Sun, Y. Tian, Y. Zhu, J. Li, X. Mu and J. Xu, *Adv. Mater.*, 2018, **30**, 180469–180476.
11 T. Ben, C. Pei, D. Zhang, J. Xu, F. Deng, X. Jing and S. Qiu, *Energy Environ. Sci.*, 2011, **4**, 3991–3999.
12 J. F. Van Humbeck, T. M. McDonald, X. Jing, B. M. Wiers, G. Zhu and J. R. Long, *J. Am. Chem. Soc.*, 2014, **136**, 2432–2440.
13 S. T. Garibay, S. J.; Mondloch, J. E.; Colon, Y. J.; Farha, O. K.; Hupp, J. T.; Ngyuen, *CrystEngComm*, 2013, **3**, 1515–1519.
14 A. Comotti, F. Castiglioni, S. Bracco, J. Perego, A. Pedrini, M. Negroni and P. Sozzani, *Chem. Commun.*, 2019, **55**, 8999–9002.
15 Q. Sun, B. Aguila, Y. Song and S. Ma, *Acc. Chem. Res.*, 2020, **53**, 812–821.
16 A. A. Uliana, N. T. Bui, J. Kamcev, M. K. Taylor, J. J. Urban and J. R. Long, *Science.*, 2021, **372**, 296–299.
17 J. Kamcev, M. K. Taylor, D. M. Shin, N. N. Jarenwattananon, K. A. Colwell and J. R. Long, *Adv. Mater.*, 2019, **31**, 1808027.
18 Q. Wang, H. Gao, Q. Cui, K. Wu, F. Hao, J. Yu, Y. Zhao and Y. U. Kwon, *J. Solid State Electrochem.*, 2019, **23**, 657–666.
19 B. Guo, T. Ben, Z. Bi, G. M. Veith, X. G. Sun, S. Qiu and S. Dai, *Chem. Commun.*, 2013, **49**, 4905–4907.
20 D. M. Shin, J. E. Bachman, M. K. Taylor, J. Kamcev, J. G. Park, M. E. Ziebel, E. Velasquez, N. N. Jarenwattananon, G. K. Sethi, Y. Cui and J. R. Long, *Adv. Mater.*, 2020, **32**, 1905771.
21 E. Ghasemiestahbanati, A. Shehzad, K. Konstas, C. J. Setter, L. A. O'Dell, M. Shaibani, M. Majumder and M. R. Hill, *J. Mater. Chem. A*, 2022, **10**, 902–911.
22 P. Kaur, J. T. Hupp and S. T. Nguyen, *ACS Catal.*, 2011, **1**, 819–835.
23 Z. Xie, C. Wang, K. E. DeKrafft and W. Lin, *J. Am. Chem. Soc.*, 2011, **133**, 2056–2059.
24 Y. Yuan, Y. Yang, M. Faheem, X. Zou, X. Ma, Z. Wang, Q. Meng, L. Wang, S. Zhao and G. Zhu, *Adv. Mater.*, 2018, **30**, 1800069.
25 Y. Yang, T. Wang, X. Jing and G. Zhu, *J. Mater. Chem. A*, 2019, **7**, 10004–10009.
26 X. Yang, S. Yao, M. Yu and J. X. Jiang, *Macromol. Rapid Commun.*, 2014, **35**, 834–839.
27 A. Trewin and A. I. Cooper, *Angew. Chemie - Int. Ed.*, 2010, **49**, 1533–1535.
28 T. Yamamoto, S. Wakabayashi and K. Osakada, *J. Organomet. Chem.*, 1992, **428**, 223–237.
29 A. J. Sicard and R. T. Baker, *Org. Process Res. Dev.*, 2020, **24**, 2950–2952.
30 T. Yamamoto, K. Osakada, T. Wakabayashi and A. Yamamoto, *Die Makromol. Chemie, Rapid Commun.*, 1985, **6**, 671–674.
31 N. Saito and T. Kanbara, *Macromolecules*, 1994, **27**, 756–761.
32 T. Yamamoto, *Appl. Organomet. Chem.*, 2014, **28**, 598–604.
33 W. Lu, D. Yuan, J. Sculley, D. Zhao, R. Krishna and H. Zhou, *J. Am. Chem. Soc.*, 2011, **133**, 18126–18129.
34 D. A. Everson and D. J. Weix, *J. Org. Chem.*, 2014, **79**, 4793–4798.
35 L. L. Anka-Lufford, K. M. M. Huihui, N. J. Gower, L. K. G. Ackerman and D. J. Weix, *Chem. - A Eur. J.*, 2016, **22**, 11564–11567.
36 P. Fayon and A. Trewin, *Phys. Chem. Chem. Phys.*, 2016, **18**, 16840–16847.
37 K. E. Poremba, N. T. Kadunce, N. Suzuki, A. H. Cherney and S. E. Reisman, *J. Am. Chem. Soc.*, 2017, **139**, 5684–5687.
38 S. Biswas and D. J. Weix, *J. Am. Chem. Soc.*, 2013, **135**, 16192–16197.
39 A. Comotti, S. Bracco, M. Mauri, S. Mottadelli, T. Ben, S. Qiu and P. Sozzani, *Angew. Chemie - Int. Ed.*, 2012, **51**, 10136–10140.
40 Y. J. Yadav, T. F. Mastropietro, E. I. Szerb, A. M. Talarico, S. Pirillo, D. Pucci, A. Crispini and M. Ghedini, *New J. Chem.*, 2013, **37**, 1486–1493.
41 P. C. Hayes, A. Osman, N. Seudeal and D. G. Tuck, *J. Organomet. Chem.*, 1985, **291**, 1–8.
42 I. Kani, Ö. Atlier and K. Güven, *J. Chem. Sci.*, 2016, **128**, 523–536.
43 G. H. Eom, H. M. Park, M. Y. Hyun, S. P. Jang, C. Kim, J. H. Lee, S. J. Lee, S. J. Kim and Y. Kim, *Polyhedron*, 2011, **30**, 1555–1564.
44 J. Perego, D. Piga, S. Bracco, P. Sozzani and A. Comotti, *Chem. Commun.*, 2018, **54**, 9321–9324.